Structure and Dynamics of Pentaglycyl Bridges in the Cell Walls of *Staphylococcus aureus* by $^{13}C-^{15}N$ REDOR NMR

Gang Tong,[‡,§] Yong Pan,[‡,||] Hao Dong,[⊥,▽] Roger Pryor,[⊥] G. Edwin Wilson,[⊥] and Jacob Schaefer*[,‡]

Department of Chemistry, Washington University, St. Louis, Missouri 63130, and Department of Chemistry, University of Akron, Akron, Ohio 44325

Received March 4, 1997; Revised Manuscript Received May 27, 1997[⊗]

ABSTRACT: Whole cells and cell-wall fractions of *Staphylococcus aureus* have been labeled by various combinations of [1-^{13}C]glycine, [^{15}N]glycine, L-[6-^{13}C]lysine, L-[6-^{15}N]lysine, D-[1-^{13}C]alanine, and D-[^{15}N]-alanine. The resulting materials have been examined using ^{13}C and ^{15}N solid-state, magic-angle spinning NMR techniques including cross-polarization, double cross-polarization, and rotational-echo double resonance. The results of these measurements indicate that the peptidoglycan glycyl bridges are complete (five units long) and form cross-links between three-quarters of all peptide stems. The pentaglycyl bridges are immobilized in lyophilized cell-wall fractions in a compact conformation with inter-residue spacings comparable to those of an α helix. The bridges have a similar compact conformation in intact whole cells, regardless of whether the cells have been lyophilized or were hydrated and frozen at −10 °C. The bridges are also in a time-averaged compact conformation in whole cells at 0 °C but with sizable structural fluctuations associated with local mobility. A small fraction of bridges are in extended-chain conformations.

The major component of the bacterial cell wall is peptidoglycan, a cage-like macromolecule which covers the entire cell (Rogers et al., 1980). The general chemical structure of peptidoglycan is the same for all bacterial species and consists of a glycan backbone of polysaccharide chains with a repeat unit of *N*-acetylglucosamine and *N*-acetylmuramic acid linked by a $\beta(1-4)$ covalent bond. Peptide stems are attached to the *N*-acetylmuramic acid units of the backbone, and these stems differ from one species to another. The peptidoglycan of *Staphylococcus aureus* (A3α) is based on the pentapeptide stem L-Ala-D-Glu-L-Lys-D-Ala-D-Ala. Cross-linking occurs by means of pentaglycyl bridges from the carbonyl carbon of D-Ala of the fourth position of one stem to the ϵ nitrogen of L-Lys of the third position of another (Figure 1). Terminal D-Ala units of cross-linked stems are eliminated (Rogers et al., 1980). Cross-linking presumably adds to the structural integrity of the bacterial cell wall and may also affect its permeability (Ghuysen et al., 1968). Because the cell changes volume as much as 200% with changing ionic conditions (Marquis, 1968; Ou & Marquis, 1970), the cell wall must be flexible. One model of the cell wall (Barnickel et al., 1983; Leps et al., 1987) proposes that the glycan chains confer structural rigidity and that the cross-linking bridges provide flexibility by expanding under stress (see Figure 1).

Many antibacterial drugs interfere with peptidoglycan biosynthesis, cross-linking, or cell-wall transport properties (Reynolds, 1989; Labischinski et al., 1993). Perhaps it is not unreasonable to suppose that the design and testing of such drugs could be enhanced by an improved characterization of cell-wall peptidoglycan cross-linking, mobility, and potential sites of interaction for drugs. Because bacterial peptidoglycan is insoluble and heterogeneous, the two most widely used biophysical structural tools with atomic resolution, solution-state NMR and X-ray crystallography, are not applicable. In this paper, we show that the combination of the incorporation of ^{13}C and ^{15}N specific labels into the peptioglycan of *S. aureus*, and subsequent detection of the labels by solid-state NMR, is capable of specifying the structure and dynamics of the pentaglycyl cross-linking bridge in fully hydrated cells.

MATERIALS AND METHODS

S. aureus Growth on Defined Medium and Harvesting. Peptidoglycan was isolated from mid-log phase cells of *S. aureus* (ATCC 6538P) grown on a defined medium (SASM) containing the following on a per-liter basis: 10 g of D-glucose; 1 g each of $K_2HPO_4 \cdot 3H_2O$, KH_2PO_4, and $(NH_4)_2SO_4$; 0.2 g of $MgSO_4 \cdot 7H_2O$; 10 mg each of $MnSO_4 \cdot H_2O$, $FeSO_4 \cdot H_2O$, and NaCl; 5 mg each of adenine, cytosine, guanine, uracil, and xanthine; 2 mg each of calcium pantothenate, thiamine·HCl, and niacin; 1 mg each of pyridoxine·HCl, riboflavin, inositol, $CuSO_4 \cdot 5H_2O$, and $ZnSO_4 \cdot 7H_2O$; 0.1 mg each of biotin and folic acid; and 0.1 g of all 20 common amino acids. The pH was adjusted to 7.0, and the medium was filter-sterilized by passage through a 0.2 μm membrane filter. One-liter growths were performed in an Applikon two-liter bench-top fermenter (Cole-Parmer Instrument Co., Chicago, IL) operated at 37 °C with aeration and stirring. Sterile Antifoam Concentrate A was added periodically. Bacterial growth was initiated by aseptic transfer of cells from a starter culture to an absorbance of 0.01 at 660 nm. *S. aureus* cells were harvested at mid-log

* To whom correspondence should be addressed.
‡ Washington University.
§ Present address: Department of Biochemistry, Duke University Medical Center, Durham, NC 27710.
|| Present address: The Procter & Gamble Company, Corporate Research Division, Cincinnati, OH 45239.
⊥ University of Akron.
▽ Present address: Ohio Environmental Protection Agency, Columbus, OH 43215.
⊗ Abstract published in *Advance ACS Abstracts,* July 15, 1997.
[1] Abbreviations: EDTA, ethylenediaminetetraacetic acid; CP, cross-polarization; MAS, magic-angle spinning; DCP, double cross-polarization; REDOR, rotational-echo double resonance.

S0006-2960(97)00495-9 CCC: $14.00

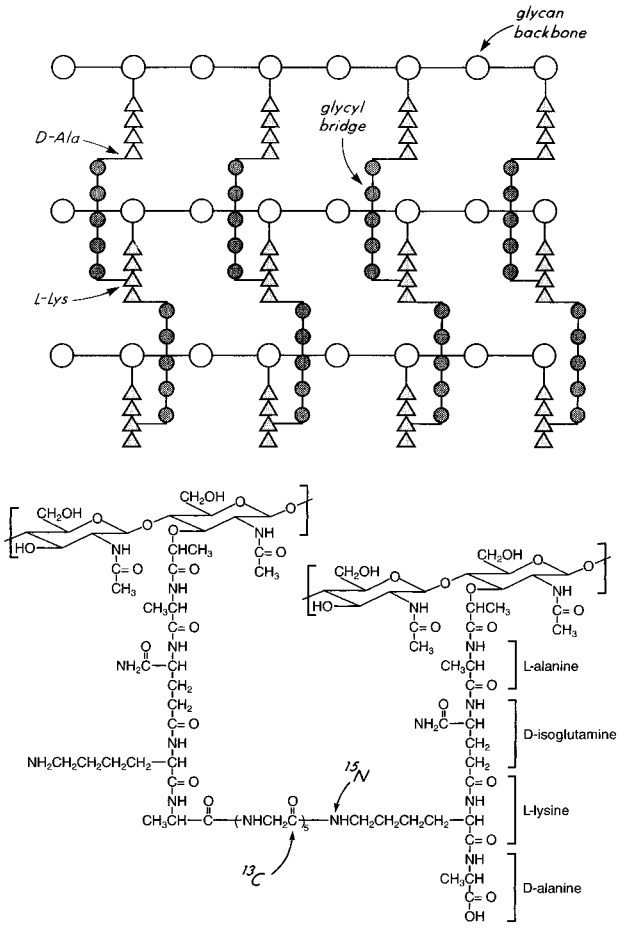

FIGURE 1: (Top) Schematic representation of an idealized version of the cell-wall peptdioglycan of *S. aureus* (after Stryer). A four-unit peptide stem (triangles) having the sequence, L-Ala-D-Glu-L-Lys-D-Ala, is attached to every second sugar of the glycan backbone (open circles). Cross-linking between glycans occurs through pentaglycyl bridges (dark circles) connecting the carbonyl carbon of D-Ala of the fourth position of one stem and the ϵ nitrogen (in an isopeptide bond) of L-Lys of the third position of another. (Bottom) Chemical structure of the peptidoglycan of *S. aureus*, with two sites identified which are suitable for stable-isotope labeling.

phase, absorbance approximately 1.0. To prepare samples for NMR spectroscopy, bacteria were grown in SASM in which the natural-abundance amino acids were replaced by L-[6-^{15}N]lysine, L-[1-^{13}C]lysine, [^{15}N]glycine, [1-^{13}C]glycine, D-[^{15}N]alanine, or D-[1-^{13}C]alanine singly or in pairs. Bacteria were harvested by centrifugation at 10000*g* for 10 min at 4 °C and washed once by resuspension in cold, sterile 0.025 M potassium phosphate buffer, pH 7.0. Washed cells were pelleted by centrifugation at 10000*g* for 15 min at 4 °C and lyophilized or used directly for preparation of cell walls or for NMR. The yield of lyophilized cells was approximately 0.3 g per liter of culture.

Peptidoglycan Isolation. Cells were suspended in 50 mL of cold, sterile 0.025 M potassium phosphate buffer containing 5 mg of DNase, pH 7.0, and disrupted in the 60 mL chamber of a Bead-Beater (Biospec Products, Bartlesville, OK) one-third full of 0.5 mm diameter glass beads at 0 °C with 10 one-minute disruption cycles separated by one-minute cooling periods. Glass beads were removed using a coarse sintered glass funnel and washed with a solution of 10 mM sodium EDTA. Centrifugation of the filtrate at 25000*g* for 30 min at 4 °C provided crude cell walls. A suspension of the crude cell wall pellet in sterile water was added dropwise with stirring to 100 mL of boiling 4% sodium dodecyl sulfate. The suspension was boiled for 30 min and was then cooled for 2 h with stirring, after which time it was allowed to stand unstirred overnight at room temperature, sedimented by centrifugation at 60000*g* for 20 min at room temperature, and washed three times with sterile, reagent grade water. The pellet was incubated at 37 °C with stirring for 16 h in 60 mL of 0.01 M TRIS buffer, pH 8.2, containing 16 mg each of trypsin and chymotrypsin and 5 mg DNase, and then sedimented by centrifugation at 100000*g* for 1 h at 20 °C and washed three times with water.

Cross-Polarization and Double Cross-Polarization. Solid-state NMR spectra were obtained with a spectrometer built around an Oxford, wide-bore superconducting solenoid operating at 4.7 T. A triple-tuned ^{1}H−^{13}C−^{15}N transmission-line probe (McKay, 1984) with a 12-mm solenoidal receiver coil was used. Cross-polarization (CP) transfers from protons to either ^{13}C or ^{15}N were made under matched spin-lock conditions at 38 kHz with magic-angle spinning (MAS) at 3205 Hz for lyophilized cell walls, and 1859 Hz for hydrated whole cells. Transfer times of 2 ms were used for all the spectra displayed in the figures. Peak intensities were corrected for proton rotating-frame relaxation by systematic variation of transfer times (Stejskal et al., 1978). Double cross-polarization (DCP) transfers (Schaefer et al., 1984a) were made with a 3-ms ^{13}C−^{15}N contact under a one-spinning speed Hartmann−Hahn frequency mismatch (38 and 35 kHz for the ^{13}C and ^{15}N rf field amplitudes, respectively, each under active control). Dipolar decoupling was performed at 95 kHz. Residual spinning sidebands were suppressed by pulse techniques (Dixon, 1982). Hydrated samples weighed 600 mg, and lyophilized samples weighed 150 mg. Hydrated samples were contained in 11-mm outside-diameter, double-bearing Kel-F rotors fitted with o-ring seals and screw-thread relief vents (Garbow et al., 1989). These rotors were not spun faster than 2 kHz to avoid plastic deformations of the barrel. Lyophilized samples were contained in zirconia rotors fitted with conventional Kel-F end and drive caps.

REDOR. Rotational-echo double resonance (REDOR) provides a direct measure of heteronuclear dipolar coupling between isolated pairs of labeled nuclei (Gullion & Schaefer, 1989a,b). In a solid with a ^{13}C−^{15}N labeled spin pair, for example, the ^{13}C rotational echoes that form each rotor period following a proton to ^{13}C cross-polarization transfer can be prevented from reaching full intensity by insertion of two ^{15}N π pulses per rotor cycle, one in the middle of the rotor period and the other at the completion of the rotor period. The pulses were applied using an *XY* phase-cycling scheme (Gullion et al., 1990; Gullion & Schaefer, 1991) to suppress offset effects and help compensate for pulse imperfections. The ^{15}N π pulse in the middle of the evolution period was replaced by a single ^{13}C π pulse to refocus isotropic chemical shifts while avoiding interference with echo formation from ^{13}C−^{13}C coupling in samples with multiple ^{13}C labels. The REDOR difference (the difference between a ^{13}C NMR spectrum obtained under these conditions and one obtained with no ^{15}N π pulses) has a strong dependence on the dipolar coupling and hence the internuclear distance (Gullion & Schaefer, 1989b). The dephasing of magnetization in REDOR arises from a local dipolar field gradient and involves no polarization transfer. REDOR has no depen-

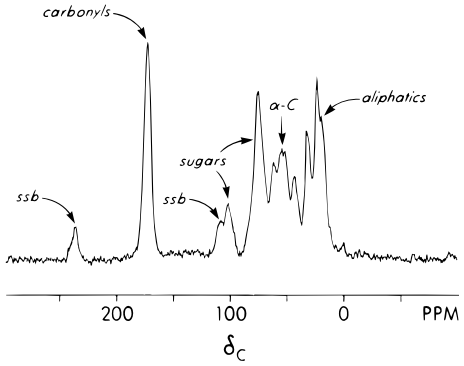

FIGURE 2: Natural-abundance CPMAS ^{13}C NMR spectrum of the cell walls of *S. aureus*. The spectrum was obtained at 50.3 MHz with 3.205-kHz magic-angle spinning.

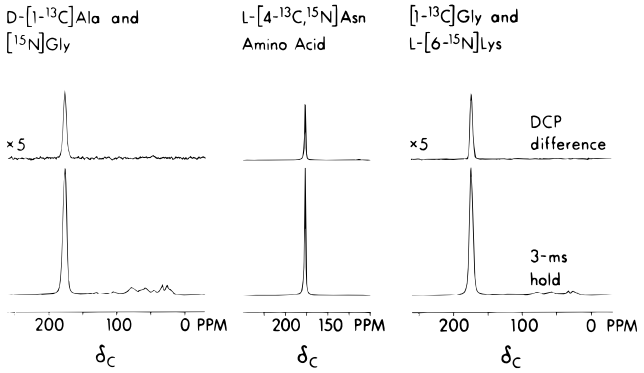

FIGURE 3: DCP ^{13}C NMR spectra of cell walls of *S. aureus* labeled by D-[1-^{13}C]alanine and [^{15}N]glycine (left) or by [1-^{13}C]glycine and L-[6-^{15}N]lysine (right). The middle spectra are of an amino-acid standard that is 90% ^{13}C enriched and 95% ^{15}N enriched. The spectra shown at the top of the figure are differences between ^{13}C signals from magnetization remaining spin-locked for 3 ms with and without a ^{15}N rf field satisfying a Hartmann−Hahn condition mismatched by the spinning speed. The spectra shown at the bottom of the figure were obtained with the 3-ms ^{13}C spin-lock but without a $^{13}C-^{15}N$ Hartmann−Hahn contact. Spinning sidebands were suppressed by pulse techniques.

dence on ^{13}C or ^{15}N chemical-shift tensors and does not require resolution of a $^{13}C-^{15}N$ coupling in the chemical-shift dimension (Marshall et al., 1990; Holl et al., 1992).

RESULTS

Isolated Cell-Wall Structure. The natural-abundance ^{13}C NMR spectrum of isolated cell walls of *S. aureus* (Figure 2) has peaks due to peptide-stem and glycan carbonyl carbons (175 ppm), sugars (100 and 60−80 ppm), peptide-stem α carbons (60 ppm), and various side chain aliphatic carbons (30 ppm). No signals from aromatic carbons are observed in the 120−150 ppm region, consistent with a largely protein-free cell-wall preparation (Forrest et al., 1991). Interpretation of spectra can therefore begin with the stoichiometry represented in Figure 1.

The double cross-polarization ^{13}C NMR spectra of cell walls isolated from *S. aureus* grown on media containing D-[1-^{13}C]alanine and [^{15}N]glycine, or containing [1-^{13}C]-glycine and L-[6-^{15}N]lysine, are shown in Figure 3. The intense 3-ms spin-lock ^{13}C signals at 175 ppm indicate massive labeling of the pentaglycyl bridge. The DCP differences for a 3-ms $^{13}C-^{15}N$ contact are 10% of the full spin-lock ^{13}C signal without $^{13}C-^{15}N$ contact for both cell-wall preparations. These DCP ratios have no dependence

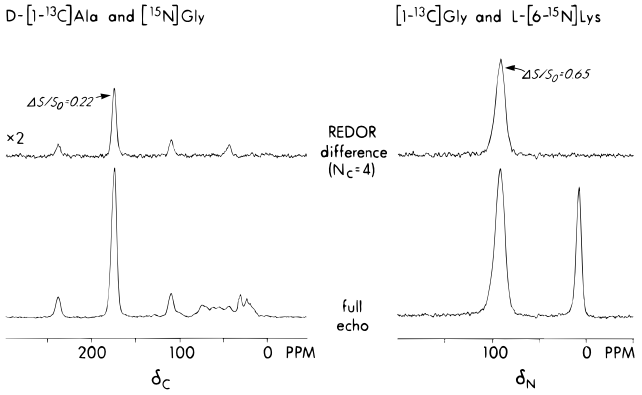

FIGURE 4: (Left) REDOR ^{13}C NMR spectra (with four rotor cycles of ^{15}N dephasing) of cell walls of *S. aureus* labeled by D-[1-^{13}C]-alanine and [^{15}N]glycine. (Right) REDOR ^{15}N NMR spectra (with four rotor cycles of ^{13}C dephasing) of cell walls labeled by [1-^{13}C]-glycine and L-[6-^{15}N]lysine. The REDOR differences are shown at the top of the figure and the full-echo spectra at the bottom. The REDOR difference is $\Delta S = S_0 - S$, where S_0 is the full-echo spectrum and S is the REDOR dephased spectrum. Because the ϵ-^{15}N lysine label is exclusively in L-Lys, the $\Delta S/S_0$ for the lysine amide-nitrogen (top right) establishes the isotopic enrichment of the glycyl carbonyl-carbons as 65%. MAS was at 3.205 kHz.

on either $T_{1\rho}(C)$ or $T_{1\rho}(N)$ (Stejskal et al., 1984). A calibration experiment (Garbow et al., 1984) on L-[4-^{13}C, *amide*-^{15}N]asparagine shows that the DCP difference for a directly bonded $^{13}C-^{15}N$ pair is 50% of the full signal (Figure 3, middle).

The ^{13}C REDOR difference after four rotor cycles of ^{15}N dephasing of the cell walls labeled by D-[1-^{13}C]alanine and [^{15}N]glycine is 22% (Figure 4, left), which is twice the DCP difference noted above (Figure 3, left). Essentially no DCP difference is expected for nonbonded $^{13}C-^{15}N$ pairs after only a 3-ms contact (Stejskal et al., 1984). Thus, the factor of 2 between DCP and REDOR measurements on the same sample establishes that the REDOR dephasing after four rotor cycles can be interpreted exclusively in terms of directly bonded $^{13}C-^{15}N$ pairs.

The ^{15}N REDOR difference after four rotor cycles of ^{13}C dephasing of the cell walls labeled by [1-^{13}C]glycine and L-[6-^{15}N]lysine is 0.65 (Figure 4, right). This measurement fixes the isotopic enrichment of the glycyl carbonyl carbons in the bridge at 65%. When the dephasing is extended to 48 rotor cycles, $\Delta S/S_0$ for the 95-ppm amide-nitrogen peak was 1, while that for the 10-ppm amine-nitrogen peak was only a few percent (data not shown). Thus, the glycyl ^{13}C carbons are dipolar coupled only to the ϵ-^{15}N nitrogen that is covalently attached to their bridge.

The CPMAS ^{15}N NMR spectrum (Shenouda et al., 1996) of the cell-wall sample labeled by [1-^{13}C]glycine and L-[6-^{15}N]lysine is shown in Figure 5 (bottom). The intense ϵ-^{15}N amide-nitrogen signal indicates that most stems are cross-linked, although the presence of a sizable ϵ-^{15}N amine peak shows that some stems are not. Non-cross-linked stems terminating in D-alanyl-D-alanine pairs are detected directly by a one-bond $^{13}C-^{15}N$ coupling in REDOR experiments performed on a sample labeled by D-[1-^{13}C]Ala and D-[^{15}N]-Ala (Figure 6, left).

Isolated Cell-Wall Bridge Conformation. Characterization of the conformation of the pentaglycine bridges is possible by REDOR NMR of cell walls labeled by [1-^{13}C]glycine and L-[6-^{15}N]lysine. We assume that the ^{13}C full-echo

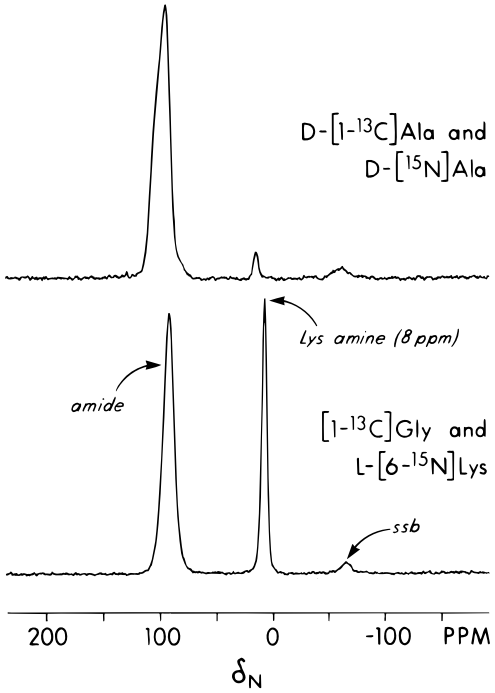

FIGURE 5: CPMAS ^{15}N NMR spectra of cell walls of *S. aureus* labeled by D-[1-^{13}C]alanine and D-[^{15}N]alanine (top), or [1-^{13}C]-glycine and L-[6-^{15}N]lysine (bottom). Unique ^{15}N chemical shifts (measured relative to external ammonium sulfate) for each label indicate the absence of scrambling. The high-field spinning sideband (ssb) for the amide peaks appear at −60 ppm. The spectra were obtained at 20.3 MHz with 3.205-kHz MAS.

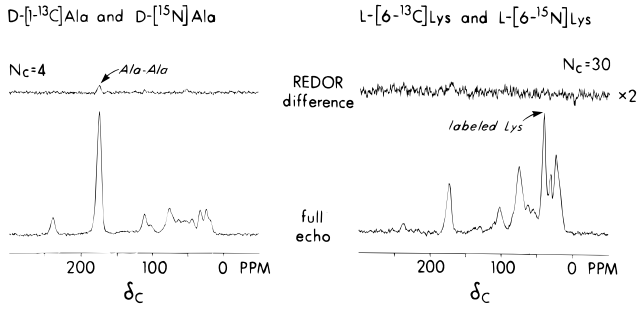

FIGURE 6: REDOR ^{13}C NMR spectra (with ^{15}N dephasing) of cell walls of *S. aureus* labeled by D-[1-^{13}C]alanine and D-[^{15}N]alanine (left) or by L-[6-^{13}C]lysine and L-[6-^{15}N]lysine (right). The REDOR differences are shown at the top of the figure, and the full-echo spectra is at the bottom. The REDOR difference is $\Delta S = S_0 - S$, where S_0 is the full-echo spectrum and S is the REDOR dephased spectrum. MAS was at 3.205 kHz.

REDOR signal is due to five glycyl carbonyl carbons, one of which is directly bonded to the 100% ^{15}N-enriched ϵ nitrogen of the cross-linking lysyl side chain. Thus, the directly bonded $^{13}C-^{15}N$ pair accounts for the REDOR difference of 0.2 (relative to the full-echo intensity) after four rotor cycles of dephasing with 3.205-kHz magic-angle spinning (Figure 7, right). This result is consistent with that of the DCP experiment on the same sample (Figure 3, right). The REDOR difference grows to about 0.6 after only 48 rotor cycles, which indicates that most of the glycyl carbonyl labels are within 5 Å (Marshall et al., 1990) of the cross-linked lysyl ^{15}N-labeled side chain. That is, the glycyl bridges must be in a compact conformation.

Information about the glycyl bridges is also available from ^{15}N REDOR experiments performed on cell walls labeled by D-[1-^{13}C]alanine and [^{15}N]glycine (Figure 7, left). The

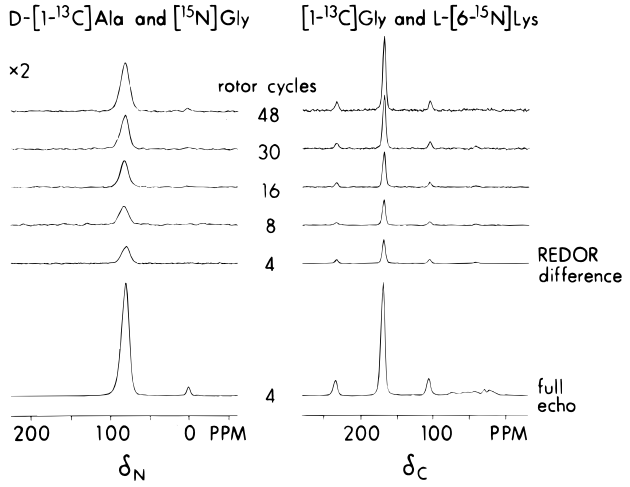

FIGURE 7: (Left) REDOR ^{15}N NMR spectra (with ^{13}C dephasing) of cell walls of *S. aureus* labeled by D-[1-^{13}C]alanine and [^{15}N]-glycine. The REDOR differences are shown as a function of the number of rotor cycles of dephasing. The full-echo spectrum after four rotor cycles with no dephasing is at the bottom of the figure. The REDOR differences have been scaled so that $\Delta S/S_0$ is determined by comparison to the full-echo signal for $N_c = 4$. (Right) REDOR ^{13}C NMR spectra (with ^{15}N dephasing) of cell walls labeled by [1-^{13}C]glycine and L-[6-^{15}N]lysine. Both left and right sets of spectra were obtained with 3.205-kHz MAS.

characteristic 80-ppm shift of the glycyl amide-nitrogen peak confirms the absence of scrambling of glycyl ^{15}N label, while the minor glycyl amine-peak intensity indicates that most bridges are complete and cross-linked. Assuming that the bridges are indeed five units long and terminated by a D-Ala-Gly covalent bond, the 10% $\Delta S/S_0$ ($N_c = 4$) means that the isotopic enrichment for D-[1-^{13}C]alanine is 50%. No significant dipolar coupling is observed between ^{13}C and ^{15}N lysine labels on different stems (Figure 6, right), or between bridges and stems not covalently attached (see Figure 4, right; in addition, no amine-nitrogen dephasing was observed for $N_c = 48$), so no inter-stem or inter-bridge-stem dipolar coupling needs be considered in the quantitative analysis of the long-range REDOR dephasing of Figure 7.

Whole Cells. The CPMAS ^{13}C NMR spectrum of fully hydrated cells of *S. aureus*, labeled by [1-^{13}C]glycine and L-[6-^{15}N]lysine and frozen at −10 °C, is shown in Figure 8 (top). In addition to the glycyl carbonyl centerband and pronounced sidebands from the 1.859-kHz magic-angle spinning, an aromatic-carbon peak near 150 ppm is observed, which we attribute to the routing of glycyl label into purines (Jacob et al., 1985) for cells undergoing active metabolism. The carbonyl-carbon sidebands decrease in intensity, and the centerband sharpens with increasing temperature (Figure 8, bottom). These spectral changes were fully reversible with the cycling of sample temperature. The integrated intensities of the CPMAS spectra at −10 and +5 °C were 40% and 10%, respectively, of that of the same sample after lyophilization. These intensity comparisons had rotating-frame and laboratory-frame relaxation rates taken into account (Stejskal et al., 1978). The ratio of the REDOR difference to full-echo signal intensity is the same for two different whole-cell samples, one lyophilized and the other frozen after extended temperature cycling indicating no substantive change in structure (Figure 9).

At +5 °C, the labeled glycyl, carbonyl-carbon REDOR full-echo peak is partially resolved, with a major resonance

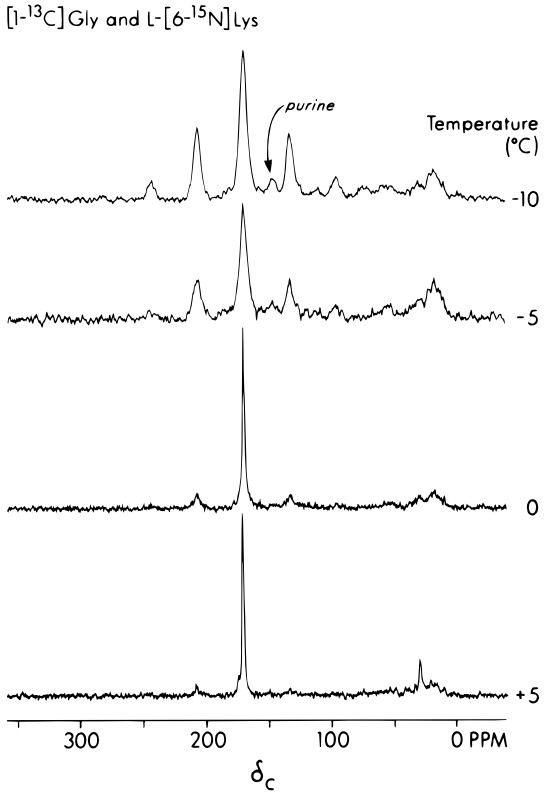

FIGURE 8: CPMAS ^{13}C NMR spectra of hydrated whole cells of *S. aureus* labeled by [1-^{13}C]glycine and L-[6-^{15}N]lysine as a function of temperature. The spinning speed was 1.859 kHz.

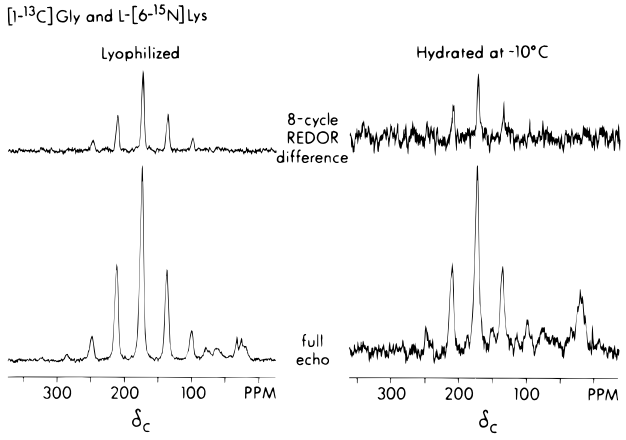

FIGURE 9: REDOR ^{13}C NMR spectra (with ^{15}N dephasing) of whole cells of *S. aureus* labeled by [1-^{13}C]glycine and L-[6-^{15}N]lysine that were lyophilized (left) or were fully hydrated and frozen at −10 °C (right). REDOR differences are at the top of the figure and full-echo spectra at the bottom. MAS was at 1.859 kHz.

at 173 ppm and a shoulder at 172 ppm (Figure 10, bottom left). The REDOR difference signal is primarily associated with the high-field shoulder (Figure 10, top left). The REDOR full-echo peak following a $\pi/2$ ^{13}C inspection pulse (*i.e.*, no cross-polarization transfer from protons to carbons preceding REDOR evolution) has the same shape but has twice the integrated intensity of the corresponding CPMAS spectrum (Figure 10, bottom right). A minor carbonyl-carbon peak at 168 ppm is also present. The corresponding REDOR difference signal (Figure 10, top right) is equal in absolute intensity to the REDOR difference of the CPMAS experiment.

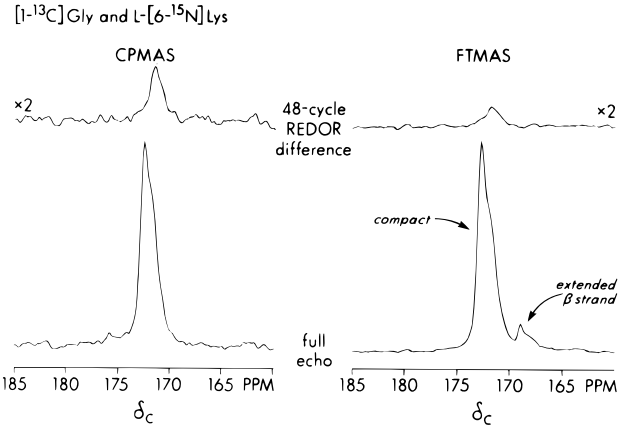

FIGURE 10: REDOR ^{13}C NMR spectra (with ^{15}N dephasing) of whole cells of *S. aureus* labeled by [1-^{13}C]glycine and L-[6-^{15}N]-lysine and hydrated at +5 °C. The spectra on the left were obtained following a cross-polarization transfer from protons to carbons, and those on the right were obtained following a ^{13}C inspection pulse. REDOR differences are at the top of the figure and full-echo spectra at the bottom. MAS was at 1.859 kHz.

DISCUSSION

Cross-Linking of Peptide Stems. The 10% DCP ratio (Figure 3, right) and the 20% 4-cycle REDOR $\Delta S/S_0$ (Figure 7, right) for the cell walls labeled by [1-^{13}C]glycine and L-[6-^{15}N]lysine mean that every pentaglycyl bridge terminates in a link with L-lysine. However, we know from the results of CPMAS ^{15}N NMR experiments on this sample (Figure 5, bottom) that not all of the peptide stems are cross-linked. The amide to amine ratio of signal intensities for the cell walls labeled by [1-^{13}C]glycine and L-[6-^{15}N]lysine is 2.7. After taking into account rotating-frame relaxation rates (Pan et al., 1993), and the intensities of spinning sidebands, this ratio is corrected to 3.0. Each lysine side chain that forms a cross-link increases the amide signal intensity and decreases the amine signal intensity by an equal amount. Thus, for the corrected ratio of amide to amine signal intensities,

$$I_{\text{amide}}/I_{\text{amine}} = \rho/(1-\rho) = 3.0$$

and $\rho = 0.75$, where ρ is the cross-link index (Forrest et al., 1991), which is the fraction of lysines whose ϵ nitrogens are part of an isopeptide bond (Figure 1).

D-Ala-D-Ala Terminated Stems. If one-fourth of the peptide stems are not cross-linked, we anticipate that about one-fourth of them are terminated by D-Ala-D-Ala pairs (Reynolds, 1989). We can confirm this expectation from a measurement of the direct coupling between D-[^{15}N]alanine and D-[1-^{13}C]alanine. This coupling produces a REDOR difference of about 5% (Figure 6, left), ignoring contributions to ΔS from natural-abundance ^{13}C in stem carbonyls adjacent to ^{15}N labels. When we assume that the isotopic incorporation for each alanine label is half the 50% value observed for the cell walls labeled by D-[1-^{13}C]alanine and [^{15}N]glycine (Figure 7, bottom left), and if we also assume no scrambling of label, the corrected REDOR dephasing for Figure 6 (left) is

$$\Delta S/S_0 = (f)(\text{D-[}^{15}\text{N]alanine isotopic enrichment})/(1+f)$$

where f is the fraction of peptide stems ending in D-Ala-D-Ala. This expression takes into account the four combinations of ^{13}C and ^{15}N labels which appear in the fraction (f)

of stems ending in D-Ala-D-Ala pairs (only one of which produces a REDOR difference), the two possibilities for ^{13}C and ^{15}N in the fraction $(1 - f)$ of stems ending in a single D-Ala, and the appearance of single ^{13}C and ^{15}N labels in both four- and five-residue stems. The observed $\Delta S/S_0$ leads to a value for f of 0.25, which is in agreement with the $1-\rho$ obtained from Figure 5 and is consistent with the notion that stems which are not cross-linked end in D-Ala-D-Ala.

A second, independent determination of the concentration of peptide stems ending in D-Ala-D-Ala is based on the REDOR dephasing of the cell-wall sample labeled by D-[1-^{13}C]alanine and [^{15}N]glycine (Figure 4, left). For this labeling, a directly bonded $^{13}C-^{15}N$ pair which will contribute to the ^{13}C ΔS is present when a cross-link is formed and the terminal alanine eliminated. If the cross-link is not formed, both D-Ala-D-Ala units of the stem contribute to S_0. Thus, if the alanine label is not scrambled:

$$\Delta S/S_0 = (1 - f)(\text{D-[}^{15}\text{N]glycine isotopic enrichment})/(1 + f)$$

We estimate the ^{15}N isotopic enrichment in the pentaglycyl bridge at 50%, the value established for the corresponding ^{13}C enrichment of the carbonyl carbon, and measure $\Delta S/S_0$ as about 0.2 (Figure 4, left). Thus, $f \approx 0.4$, which also is reasonably close to $1 - \rho$. We conclude that all pentaglycyl bridges are complete and part of inter-stem cross-links and that peptide stems not cross-linked terminate in D-Ala-D-Ala.

Both of these assessments of the fraction of stems ending in D-Ala-D-Ala are, however, only semiquantitative because we have ignored the racemization of label in D-Ala to L-Ala, which affects S_0. The quantitation can be improved either by additional labeling experiments using double-labeled alanines to determine isotopic specific activities (Pan et al., 1993) or by combining mass spectrometric determinations of isotopic enrichment of D and L cell-wall amino acids following digestion and chromatographic separation (Forrest et al., 1991). Combining mass spectrometric and NMR results would also provide experimental verification of glycyl bridge length and determination of the concentration of D-Ala-Gly stem-bridge covalent bonds.

Quantitation and Spin Counting for Hydrated Whole Cells. The CPMAS ^{13}C NMR total integrated intensity of the hydrated whole cells (at −10 °C) labeled by [1-^{13}C]glycine and L-[6-^{15}N]lysine is only 40% of that of the same sample after lyophilization (data not shown). At −10 °C, the hydrated sample is a soft-frozen paste. We believe that 60% of the signal is not observed at −10 °C because some regions of the frozen paste have large-amplitude, 50-kHz-regime reorientational dynamic fluctuations which involve segments of cell walls, attached proteins, and associated cytoplasmic proteins. This kind of lost signal intensity in heterogeneous, solid-like preparations has been noted before for bacterial whole cells (Garbow et al., 1989), protein complexes in buffer glasses (McDowell et al., 1996), and plasticized synthetic polymer blends (Schaefer et al., 1987). The observable carbonyl-carbon signal has a broad spinning sideband pattern indicating that at least for those carbons reporting in the frozen paste, the chemical-shift tensor is not averaged by large-amplitude motion faster than 10 kHz (Schaefer et al., 1984b).

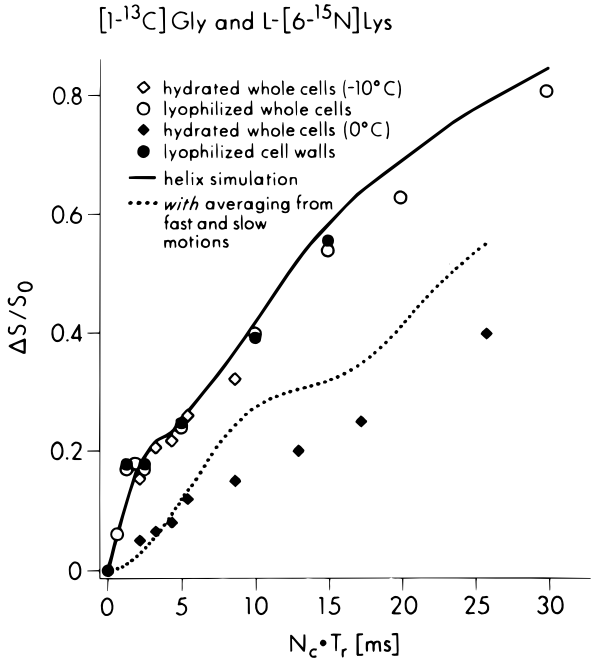

FIGURE 11: REDOR dephasing ($\Delta S/S_0$) as a function of the REDOR evolution time (N_cT_r) for whole cells and cell walls of *S. aureus* labeled by [1-^{13}C]glycine and L-[6-^{15}N]lysine. Results for lyophilized samples are represented by circles, and results for hydrated samples are represented by diamonds. The calculated dephasing is based on the parameters of Table 1.

As the temperature increases, more and more motion reduces the $^1H-^{13}C$ dipolar coupling needed for an effective cross-polarization transfer, and the carbonyl-carbon CPMAS signal intensity decreases. At the same time, high-frequency motion shortens relaxation times and makes rotor-synchronized Hahn-echo detection practical following a single ^{13}C $\pi/2$ inspection pulse. At 5 °C, the ^{13}C T_1-relaxed spectrum (which was obtained with ^1H dipolar decoupling) has twice the integrated intensity of the corresponding CPMAS spectrum at 5 °C and half the intensity of the CPMAS spectrum of the frozen cells. Because no Overhauser enhancement is present in this kind of single-pulse experiment (Noggle & Schirmer, 1971), the Fourier-transform spectrum at +5 °C, and the CPMAS spectrum of the frozen cells, probably arise from the same number of labeled carbonyl carbons.

REDOR Dephasing and Conformation of the Pentaglycyl Bridge. The dependence of the REDOR dephasing ($\Delta S/S_0$) on the total evolution time (Gullion & Schaefer, 1989b) is shown in Figure 11 for lyophilized cell walls and for lyophilized and hydrated whole cells, labeled by [1-^{13}C]-glycine and L-[6-^{15}N]lysine. Because the $^{13}C-^{15}N$ pair detected by REDOR is for an isopeptide bond occuring only in cross-links of peptidoglycan (the ϵ-^{15}N lysyl label does not scramble), whole-cell REDOR spectra have the same selectivity as cell-wall REDOR spectra. Except for the $\Delta S/S_0$ of the hydrated whole cells at 0 °C, the observed dephasings are those of a compact conformation (Labischinski et al., 1993) with the five carbonyl-carbon to ϵ-nitrogen $^{13}C-^{15}N$ distances comparable to those of an α helix (Table 1). The observed $\Delta S/S_0$ would be equally well matched by couplings calculated for a 3_1 helix, which is more likely for glycine-rich peptides (Saitô, 1986). However, an extended β-strand conformation, with carbon−nitrogen distances of up to 15 Å, can only account for some 30% total dephasing (Hirsh et al., 1996), whereas almost 80% dephasing is

Table 1: REDOR Dephasing Parameters for the Pentaglycine Bridge of *S. aureus* Labeled by [1-^{13}C]Glycine and L-[6-^{15}N]Lysine

position of glycyl unit relative to lysine ϵ nitrogen	distance from glycyl carbonyl carbon to lysine nitrogen[a] (Å)	static dipolar coupling (Hz)	reduced dipolar coupling, one fast motion[b] (Hz)	reduced dipolar coupling, one fast and one slow motion[c] (Hz)
1	1.35	1220	153	153
2	3.26	86	73	34
3	3.70	59	52	31
4	4.01	46	42	28
5	5.89	15	14	14

[a] Inter-unit spacings for an α helix. [b] Dipolar coupling scaled by $1 - 3\langle\sin^2\theta\rangle/2 = 0.12$ for the glycyl unit directly bonded to the L-lysyl side chain. The motional averaging is due to restricted isotropic reorientation of the ^{13}C−^{15}N internuclear vector on a sphere, where $\theta = 70°$ is the deviation of the tensor axes from equilibrium. The bracket indicates a powder average. The scaling estimate is based on a reduction of the difference in principal components of the carbonyl-carbon chemical-shift tensor ($\nu_{33} - \nu_{11}$) from 7.6 to 1.0 kHz [see Figure 8 and Herzfeld and Berger (1980)]. The dipolar couplings for the other four glycyl bridge units were scaled by assuming ±1 Å displacements of the carbonyl carbons relative to the ϵ nitrogen of the lysyl side chain. [c] Dipolar coupling scaled by $^1/_8$ for the glycyl unit directly bonded to L-Lys. The dipolar couplings for the middle three glycyl bridge units were scaled by assuming 2-Å displacements of the carbonyl carbons relative to the ϵ-nitrogen of lysine, associated with isotropic reorientation of the ^{13}C−^{15}N vector on a sphere.

observed. Thus we can conclude that the average bridge conformation is not extended, although we are unable to determine what kind of compact conformation the bridge is in. The fact that five ^{13}C−^{15}N couplings are needed to fit the $\Delta S/S_0$ dephasing is consistent with complete glycyl bridges. The hydrated whole cells at 0 °C have about half the $\Delta S/S_0$ dephasing of the frozen whole cells. We attribute the reduction in dephasing to an increase in bridge motion and will discuss this motion in the next section.

The REDOR differences for the hydrated whole cells at 5 °C (Figure 10, top) are associated with the high-field shoulders of the S_0 peaks. Both the central S_0 line and its shoulder have comparably reduced chemical-shift spinning sidebands (Figure 8, bottom). In the presence of this motional averaging of dipolar coupling, the observed REDOR differences for the shoulders are too large ($\Delta S/S_0 \approx 0.5$) to arise from carbonyl carbons from the full pentaglycyl bridge. Instead, we assign the shoulders to carbonyl carbons closest to the ϵ-^{15}N cross-link sites for all bridges. The minor peak at 168 ppm (Figure 10, bottom right) may be due to glycyl carbonyl-carbons in highly mobile, extended-chain conformations. Carbonyl-carbon shifts of 168 ppm for glycyl residues in β-sheet conformations have been observed in both solution (Wishart & Sykes, 1994) and solid-state spectra (Saitô, 1986). Experiments to induce changes in the cell-wall physical state that correlate with the intensity of the 168-ppm peak are in progress.

Local Motion of the Bridge. The extent of local motion for hydrated whole cells at 0 °C is estimated by the decrease in intensity of the carbonyl-carbon chemical-shift spinning sidebands. Assuming that the tensor is averaged by restricted isotropic reorientation on a sphere (Schaefer et al., 1984b) at a rate faster than 10 kHz, the reduction is given by the factor $1 - 3\langle\sin^2\theta\rangle/2$, where θ is the deviation of the tensor axes from their equilibrium positions. The bracket indicates a powder average (*i.e.*, $\langle\sin^2\pi\rangle = {}^2/_3$). A value of θ of about 70° will decrease the sideband intensity by a factor of 8 (Herzfeld & Berger, 1980). Angular excursions of this size correspond to atomic displacements from equilibrium of a carbonyl carbon of about ±1 Å relative to the ϵ-nitrogen of lysine.

Because the carbonyl-carbon−ϵ-nitrogen dipolar tensor has a principal axis that is co-linear with the carbonyl-carbon shift tensor, 1-Å displacements will also reduce the directly bonded ^{13}C−^{15}N dipolar coupling by a factor of 8 (Table 1). However, similar displacements for more distant carbonyl carbons have a much smaller effect on couplings because of the smaller angle subtended relative to the lysine ^{15}N. The net result is that the dependence of the REDOR dephasing on evolution time in the presence of motion faster than 10 kHz is described for only about the first 5 ms (simulation not shown).

We believe that additional motions at rates much less than 10 kHz are present for bridge reorientations as a whole. These motions could average weak, long-range ^{13}C−^{15}N dipolar couplings but not have much effect on the much larger carbonyl-carbon chemical-shift tensors. If we assume that both ends of the bridge are tied by covalent bonds to the stems, but that carbonyl carbons in the three middle glycyl bridge units have double the 1-Å displacement of the carbonyl carbons in the end glycyl units, then a reasonable fit to the dephasing behavior can be calculated for 20 ms of dephasing (Figure 11, dotted line). The long-range dipolar couplings that went into this calculation are presented in Table 1 (column five). Regardless of the details of this oversimplified description of motional averaging, the fact remains that despite extensive motion for the hydrated whole cells at 0 °C, almost half of the REDOR dephasing that is associated with lyophilized cell walls is still observed for the hydrated whole cells. We conclude that although extension of the cell-wall peptidoglycan may occur under stress from increased osmotic pressure, the time-averaged equilibrium peptidoglycan conformation for at least 90% of the hydrated cell walls is compact, not extended (Figure 10, bottom right). The remaining 10% may be in a more flexible, extended conformation and the two populations could be in slow exchange.

ACKNOWLEDGMENT

R.P. was the recipient of a Patricia Roberts Harris Fellowship. The authors thank C. A. Klug (Stanford University) for helpful suggestions. This work was supported by NSF Grant DMB 8803687 (G.E.W.) and NIH grant GM51554 (J.S.).

REFERENCES

Barnickel, G., Labischinski, H., Bradaczek, H., & Giesbrecht, P. (1979) *Eur. J. Biochem. 95,* 157−165.

Dixon, W. T. (1982) *J. Chem. Phys. 77,* 1800−1809.

Forrest, T. M., Wilson, G. E., Pan, Y., & Schaefer, J. (1991) *J. Biol. Chem. 266,* 24485−24491.

Garbow, J. R., Jacob, G. S., Stejskal, E. O., & Schaefer, J. (1989) *Biochemistry 28,* 1362−1367.

Ghuysen, J.-M., Strominger, J. L., & Tipper, D. J. (1968) in *Comprehensive Biochemistry* (Florkin, M., & Stotz, E. H., Eds.) Vol. 26A, pp 53−104, Elsevier, New York.
Gullion, T., & Schaefer, J. (1989a) *J. Magn. Reson. 81*, 196−200.
Gullion, T., & Schaefer, J. (1989b) *Adv. Magn. Reson. 13*, 57−83.
Gullion, T., & Schaefer, J. (1991) *J. Magn. Reson. 92*, 439−442.
Gullion, T., Baker, D. B., & Conradi, M. S. (1990) *J. Magn. Reson. 89*, 479−484.
Herzfeld, J., & Berger, A. E. (1980) *J. Chem. Phys. 73*, 6021−6030.
Hirsh, D. J., Hammer, J., Maloy, W. L., Blazyk, J., & Schaefer, J. (1996) *Biochemistry 35*, 12733−12741.
Holl, S. M., Marshall, G. R., Beusen, D. D., Kociolek, K., Redlinski, A. S., Leplawy, M. T., McKay, R. A., Vega, S., & Schaefer, J. (1992) *J. Am. Chem. Soc. 114*, 4830−4833.
Jacob, G. S., Schaefer, J., Stejskal, E. O., & McKay, R. A. (1985) *J. Biol. Chem. 260*, 5899−5905.
Labischinski, H., Hochberg, M., Sidow, T., Maidhof, H., Henze, U., Berger-Bächi, B., & Weche, J. (1993) in *Bacterial Growth and Lysis: Metabolism and Structure of the Bacterial Sacculus* (DePedro, M. A., Höltje, J. V., & Löffelhardt, W., Eds.) pp 9−28, Plenum, New York.
Leps, B., Labischinski, H., & Bradaczek, H. (1987) *Biopolymers 26*, 1391−1406.
Marquis, R. E. (1968) *J. Bacteriol. 95*, 775−781.
Marshall, G. R., Beusen, D. D., Kociolek, K., Redlinski, A. S., Leplawy, M. T., Pan, Y., & Schaefer, J. (1990) *J. Am. Chem. Soc. 112*, 963−966.
McDowell, L. M., Schmidt, A., Cohen, E. R., Studelska, D. R., & Schaefer, J. (1986) *J. Mol. Biol. 256*, 160−171.
McKay, R. A. (1984) U.S. Patent 4,446,431.
Noggle, J. H., & Schirmer (1971) *The Nuclear Overhauser Effect*, Academic Press, New York.
Ou, L.-T., & Marquis, R. E. (1970) *J. Bacteriol. 101*, 92−101.
Pan, Y., Shenouda, N. S., Wilson, G. E., & Schaefer, J. (1993) *J. Biol. Chem. 268*, 18692−18695.
Reynolds, P. E. (1989) *Eur. J. Clin. Microbiol. Infect. Dis. 8*, 943−950.
Rogers, H. J., Perkins, H. R., & Ward, J. B. (1980) *Microbial Cell Walls and Membranes*, Chapman and Hall, London.
Saitô, H. (1986) *Magn. Reson. Chem. 24*, 835−853.
Schaefer, J., Stejskal, E. O., Garbow, J. R., & McKay, R. A. (1984a) *J. Magn. Reson. 59*, 150−156.
Schaefer, J., Stejskal, E. O., McKay, R. A., & Dixon, W. T. (1984b) *Macromolecules 17*, 1479−1489.
Schaefer, J., Garbow, J. R., Stejskal, E. O., & Lefelar, J. A. (1987) *Macromolecules 20*, 1271−1278.
Shenouda, N. S., Pan, Y., Schaefer, J., & Wilson, G. E. (1996) *Biochim. Biophys. Acta 1289*, 217−220.
Stejskal, E. O., Schaefer, J., & Steger, T. R. (1978) *Faraday Symp. Chem. Soc. 13*, 56−62.
Stejskal, E. O., Schaefer, J., & McKay, R. A. (1984) *J. Magn. Reson. 57*, 471−485.
Wishart, D. S., & Sykes, B. D. (1994) *Methods Enzymol. 239*, 363−392.

BI970495D